Physics Letters B 760 (2016) 335–340

Contents lists available at ScienceDirect

Physics Letters B

www.elsevier.com/locate/physletb

On exclusive $h \to V\ell^+\ell^-$ decays

Pietro Colangelo [a], Fulvia De Fazio [a,*], Pietro Santorelli [b,c]

[a] INFN, Sezione di Bari, via Orabona 4, I-70126 Bari, Italy
[b] Dipartimento di Fisica "Ettore Pancini", Università di Napoli Federico II, Complesso Universitario di Monte Sant'Angelo, Via Cintia, Edificio 6, I-80126 Napoli, Italy
[c] INFN, Sezione di Napoli, I-80126 Napoli, Italy

ARTICLE INFO

Article history:
Received 8 February 2016
Received in revised form 21 June 2016
Accepted 2 July 2016
Available online 9 July 2016
Editor: B. Grinstein

ABSTRACT

We study a set of exclusive decay modes of the Standard Model Higgs boson into a vector meson and a dilepton pair: $h \to V\ell^+\ell^-$, with $V = \Upsilon, J/\psi, \phi$, and $\ell = \mu, \tau$, determining the decay rates, the dilepton mass spectra and the V longitudinal helicity fraction distributions. In the same framework, we analyze the exclusive modes into neutrino pairs $h \to V\nu\bar{\nu}$. We also discuss the implications of the recent CMS and ATLAS results for the lepton flavor-changing process $h \to \tau^+\mu^-$ on the $h \to V\tau^+\mu^-$ decay modes.

Precision tests of the properties of the Higgs-like scalar with $m_h = 125.7(4)$ GeV observed at the LHC [1–3], to verify that the Standard Model (SM) predictions for the Higgs boson are exactly fulfilled, represent an issue of prime interest in present-day theoretical and experimental activity. Particularly important is to confirm that the couplings of the observed state to the fermions and gauge bosons are what the SM dictates. The LHC measurements are consistent with the Standard Model predictions for the Higgs couplings to top and beauty quarks and to τ leptons [4], while the couplings to the other quarks and leptons are experimentally less known. Approaches based on the effective field theory which includes dimension 6 operators show how such couplings could be modified, comprising also CP violating terms [5–9]. In addition, possible beyond SM lepton and quark flavor-changing Higgs couplings need to be examined. This issue is important in connection with the current $h \to \tau\mu$ searches at LHC: for such a mode the CMS Collaboration has reported $\mathcal{B}(h \to \tau\mu) = \left(0.84^{+0.39}_{-0.37}\right) \times 10^{-2}$ and the upper bound $\mathcal{B}(h \to \tau\mu) < 1.51 \times 10^{-2}$ at 95% CL [10], while the ATLAS Collaboration quotes the bound $\mathcal{B}(h \to \tau\mu) < 1.85 \times 10^{-2}$ at 95% CL [11].

Measuring the Higgs couplings to the first two generation fermions is a difficult task. Various possibilities have been studied, with particular attention to the radiative $h \to f\bar{f}\gamma$ processes. The leptonic modes $h \to \ell^+\ell^-\gamma$ (with $\ell = e, \mu$) have been considered in [12–15] and [16]. To access the Higgs couplings to the light quarks, the exclusive channels $h \to V\gamma$, with V a vector meson, have been scrutinized in [17–20], and $h \to VZ$ have been studied in [21,22]. Here, we examine the three-body exclusive Higgs decays $h \to V\ell^+\ell^-$, where $V = \Upsilon$, J/ψ, ϕ and ℓ is a light or a heavy charged lepton. There are several motivations to afford such a study. The first one is the possibility of considering, in addition to the decay rates, some distributions encoding important physical information, namely the distributions in the dilepton invariant mass squared: we shall see, for example, that the case of τ dileptons is particularly interesting. Moreover, since several amplitudes contribute to each process, one can look at kinematical configurations where the interferences are more effective, in the attempt of getting information on the various Higgs couplings. Deviations from the Standard Model can also be probed through the search of lepton flavor violating signals. All the considered modes have a clear experimental signature, although the rates are small, and can be included in the physics programme of future high luminosity facilities.

The decays $h \to V\ell^+\ell^-$ take contribution from amplitudes in which the Higgs couples to quarks, to leptons and to the gauge bosons Z and γ. In SM such couplings are $g_{hf\bar{f}} = i\dfrac{m_f}{v}$ for fermions,[1] and $g_{hZZ} = i\dfrac{2m_Z^2}{v}$ for Z ($v = 2m_W/g = (\sqrt{2}G_F)^{-1/2} = 246$ GeV is the Higgs field vacuum expectation value). The effective $\gamma\gamma$ and $Z\gamma$ Higgs couplings are described below. Fig. 1 displays the three kinds of diagrams that must be taken into account.

* Corresponding author.
E-mail address: fulvia.defazio@ba.infn.it (F. De Fazio).

[1] For the quarks we use the running masses evaluated at the Higgs mass scale $\mu \simeq m_h = 125$ GeV at NNLO in the $\overline{\text{MS}}$ scheme.

http://dx.doi.org/10.1016/j.physletb.2016.07.002

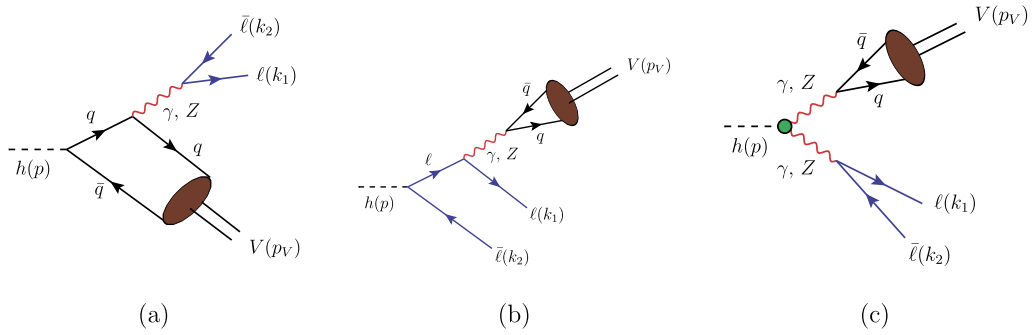

Fig. 1. Diagrams involved in $h \to V\ell^+\ell^-$ decays. In (a) and (b) the diagrams with γ and Z emitted by $\bar{q}$ and $\bar{\ell}$ are also considered. Diagram (c) represents the contribution of the $h \to ZZ$ vertex and of the effective $h \to \gamma\gamma$, $h \to \gamma Z$ vertices.

Diagrams (a) represent amplitudes with the Higgs coupled to the quark-antiquark pair. The neutral gauge boson γ or Z is emitted from the quark or the antiquark before they hadronize in the vector meson V. For low dilepton invariant mass squared $q^2 = (k_1 + k_2)^2$, the nonperturbative quark hadronization in the vector meson V can be analyzed adopting the formalism of the QCD hard exclusive processes [23–26]. The matrix elements of the non-local quark-antiquark operator, depicted in Fig. 1(a), and the vector meson can be expressed as an expansion in increasing twists, which involves various vector meson distribution amplitudes. For $V = \Upsilon,\ J/\psi,\ \phi$, the leading twist light-cone distribution amplitude (LCDA) $\phi_\perp^V$ is defined from the matrix element of the non-local $\bar{q}(y)\sigma_{\mu\nu}q(x)$ quark current:

$$\langle V(p_V,\epsilon_V)|\bar{q}(y)\sigma_{\mu\nu}q(x)|0\rangle = -f_V^\perp(\epsilon^*_{V\,\mu}p_{V\,\nu} - \epsilon^*_{V\,\nu}p_{V\,\mu})\int_0^1 du\, e^{i\,u\,p_V\cdot x + i\,\bar{u}\,p_V\cdot y}\phi_\perp^V(u) \quad (1)$$

($\bar{u} = 1-u$). $u\,p_V$ and $\bar{u}\,p_V$ represent the meson longitudinal momentum fraction carried by the quark and antiquark. $\phi_\perp^V$ is normalized to 1; the hadronic parameter $f_V^\perp$ is discussed below. The LCDA $\phi_\perp^V$ can be expressed in terms of the Gegenbauer polynomials $C_n^{3/2}$,

$$\phi_\perp^V(u,\mu) = 6u\bar{u}\left[1 + \sum_{n=1}^{\infty} a_n^{V_\perp}(\mu)C_n^{3/2}(2u-1)\right], \quad (2)$$

with the scale μ dependence of the distribution amplitude encoded in the coefficients $a_n^{V_\perp}(\mu)$. Such coefficients follow a renormalization group evolution

$$a_n^{V_\perp}(\mu) = \left[\frac{\alpha_s(\mu)}{\alpha_s(\mu_0)}\right]^{\gamma_n^\perp/(2\beta_0)} a_n^{V_\perp}(\mu_0), \quad (3)$$

where $\gamma_n^\perp = 8C_F\left(\sum_{k=1}^{n+1}\frac{1}{k} - 1\right)$, $C_F = \frac{N_c^2-1}{2N_c}$ and N_c the number of colors. We set the low-energy scale $\mu_0 \simeq 1$ GeV.

It is convenient to distinguish between the heavy $J/\psi, \Upsilon$ and light ϕ mesons. In the case of ϕ, the expansion (2) (where only the even momenta are non-vanishing) is known up to $n = 4$, with values of the coefficients [27–29]

$$a_2^{\phi_\perp}(\mu_0) = 0.14 \pm 0.07 \quad , \quad a_4^{\phi_\perp}(\mu_0) = 0.00 \pm 0.15\,. \quad (4)$$

For heavy quarkonia $V = J/\psi$ and Υ, models for LCDA have been proposed. We use the Gaussian model [29]

$$\phi_V^\perp(u,\mu_0) = N_\sigma \frac{4u\bar{u}}{\sqrt{2\pi}\sigma_V}\exp\left[-\frac{u-\frac{1}{2}}{2\sigma_V^2}\right], \quad (5)$$

with N_σ a normalization constant and the parameter σ_V, specific for each vector meson, taking the values

$$\sigma_{J/\psi} = 0.228 \pm 0.057 \quad , \quad \sigma_\Upsilon = 0.112 \pm 0.028\,. \quad (6)$$

The Gegenbauer momenta

$$a_n^{V_\perp}(\mu_0) = \frac{2(2n+3)}{3(n+1)(n+2)}\int_0^1 du\, C_n^{3/2}(2u-1)\phi_V^\perp(u,\mu_0) \quad (7)$$

are evolved using (3) to determine the distribution amplitude $\phi_V^\perp$ at the scale $\mu \sim m_h$. For J/ψ and Υ we include $n = 20$ terms in the Gegenbauer expansion.

To assess the limit of applicability of the twist expansion, we investigate the hierarchy between the leading term included in our calculation, involving the twist 2 distribution $\phi_\perp^V$ in (2), and the next-to-leading term. This involves the combination $B(u) = h_\parallel^{(t)}(u) - \frac{1}{2}\phi_\perp^V(u) - \frac{1}{2}h_3(u)$ of the distributions $h_\parallel^{(t)}$ and h_3 of twist 3 and 4, respectively [30]. While the contribution of the leading term contains the quark propagator $p_1 = 1/(m_h^2\bar{u} + uq^2 - u\bar{u}m_V^2)$, the next term involves $p_2 = m_V^2/\left(m_h^2\bar{u} + uq^2 - u\bar{u}m_V^2\right)^2$; in the case of the diagram with intermediate antiquark $u \leftrightarrow \bar{u}$ should be exchanged. The hierarchy $p_1 > p_2$ is always verified except close to the endpoint $\bar{u} = 0$ (or $u = 0$), where however the wave functions vanish. Hence, the expansion can be trusted up to quite large values of q^2.

A second issue is related to the role of $\mathcal{O}(\alpha_s)$ corrections from gluon exchanges among the quarks in the diagrams in Fig. 1(a) (they do not need to be included in the topologies when the experimental values for the decay constants f_V are used). The calculation of the corrections for $h \to V\gamma$ has been carried out at $q^2 = 0$ for a real photon [20]. An estimate of the size of the corrections in the cases considered here can be obtained extending the result to the whole q^2 range. The integrand functions in $I_1(\hat{q}^2)$ and $I_2(\hat{q}^2)$ in (23), (24) are modified as

$$I_1^{\alpha_s}(\hat{q}^2) = \int_0^1 du\,\phi_\perp^V(u)\left[\frac{1}{D_1(1-u,u,\hat{q}^2)} + \frac{1}{D_1(u,1-u,\hat{q}^2)}\right] \times\left[1 + \frac{C_F\alpha_s(\mu)}{4\pi}h(u,m_h,\mu)\right], \quad (8)$$

with [20]

$$h(u,m_h,\mu) = 2\ln[u(1-u)]\left(\log\left(\frac{m_h^2}{\mu^2}\right) - i\pi\right) + \ln^2(u) + \ln^2(1-u) - 3\,, \quad (9)$$

and similarly for I_2. The channels with larger effects are those with final Υ, where $\mathcal{O}(\alpha_s)$ corrections affect $I_{1,2}(\hat{q}^2)$ at 30% level close to $\hat{q}^2 \simeq 0$, and decrease when $\hat{q}^2$ is increased. The correction modifies the results for the rates by about 10%, as I_1 and I_2 enter in the amplitude with opposite signs.

The Higgs couplings to leptons are involved in the diagrams in Fig. 1(b), with the $q\bar{q}$ pair emitted by the photon or Z. Such diagrams are important in the case of τ. The hadronization of the $q\bar{q}$ pair into the vector meson is described by the matrix element

$$\langle V(p_V, \epsilon_V)|\bar{q}\,\gamma_\mu\, q|0\rangle = -i f_V m_V \epsilon^*_{V\,\mu}\,, \tag{10}$$

with p_V and ϵ_V the V meson momentum and polarization vector, respectively. The decay constant f_V can be extracted from the $V \to e^+e^-$ measured width. On the other hand, the hadronic parameter $f_V^\perp$ in (1) is less accessible, and results from lattice or QCD sum rule computations must be used. In our analysis we use the range for the ratio $R_{f_V} = \frac{f_V^\perp}{f_V}$ quoted in [29], obtained exploiting non-relativistic QCD scaling relations [31,32]:

$$\begin{aligned} f_\phi &= 0.223 \pm 0.0014 \text{ MeV}\,, & R_{f_\phi} &= 0.76 \pm 0.04\,, \\ f_{J/\psi} &= 0.4033 \pm 0.0051 \text{ MeV}\,, & R_{f_{J/\psi}} &= 0.91 \pm 0.14\,, \\ f_\Upsilon &= 0.6844 \pm 0.0046 \text{ MeV}\,, & R_{f_\Upsilon} &= 1.09 \pm 0.04\,. \end{aligned} \tag{11}$$

The diagrams in Fig. 1(c) involve the coupling of the Higgs to a pair of gauge bosons, which in turn are coupled to a lepton pair and to a $q\bar{q}$ pair that hadronizes into V. The elementary hZZ coupling can be read from the SM Lagrangian. The effective $h\gamma\gamma$ and $hZ\gamma$ vertices can be written as

$$A(H \to G_1 G_2) = i\frac{\alpha}{\pi v} C_{G_1G_2}\left[g_{\mu\nu}(p_V \cdot q) - p_{V\mu} q_\nu\right]\epsilon^{*\mu}_{G_1}\,\epsilon^{*\nu}_{G_2}\,, \tag{12}$$

with G_1 and G_2 either $\gamma\gamma$ or $Z\gamma$, and ϵ_{G_1}, ϵ_{G_2} polarization vectors. In Eq. (12) p_V is the momentum of the meson V and q the momentum of the dilepton. The effective $h\gamma\gamma$ and $hZ\gamma$ couplings are determined by loop diagrams: $C_{\gamma\gamma} = -3.266 + i0.021$ and $C_{\gamma Z} = -2.046 + i0.005$ [20]. In the Z propagator, the width $\Gamma(Z) = 2.4952$ GeV is included neglecting its small uncertainty [3]. It is worth remarking that the possibility to access the hZZ coupling is a feature of the class of modes we are analyzing. Moreover, since a sizeable contribution to $h \to V\ell^+\ell^-$ involves the effective $h\gamma\gamma$ and $hZ\gamma$ couplings from diagrams sensitive to New Physics effects, the exclusive processes also probe deviations from SM.

The relative role of the diagrams in Fig. 1 is different if the dilepton invariant mass is varied. At low-q^2 the amplitudes with the Higgs coupled to the quarks provide a contribution which decreases with q^2. This contribution is sizable for $\Upsilon\mu^+\mu^-$. Increasing q^2, the role of the other diagrams becomes important, and the uncertainty in the terms in Fig. 1(a) is overwhelmed by the other errors. At large q^2 the contribution is also estimated to be smaller than the uncertainty affecting the other diagrams, as one can infer modeling, e.g., the photon amplitude with the inclusion of a set of intermediate states.

To compute the branching fractions, it is necessary to get rid of the poorly known Higgs full width. One possibility is to use the expression

$$\mathcal{B}(h \to V\ell^+\ell^-) = \frac{\Gamma(h \to V\ell^+\ell^-)}{\Gamma(h \to \gamma\gamma)}\mathcal{B}(h \to \gamma\gamma)_{exp} \tag{13}$$

which employs the computed widths $\Gamma(h \to V\ell^+\ell^-)$ and $\Gamma(h \to \gamma\gamma) = \frac{\alpha^2}{64\pi^3 v^2}|C_{\gamma\gamma}|^2 m_h^3$ combined with the measurement $\mathcal{B}(h \to \gamma\gamma)_{exp} = (2.28 \pm 0.11) \times 10^{-3}$ [33]. We obtain the following results:

$$\begin{aligned} \mathcal{B}(h \to \phi\mu^+\mu^-) &= (7.93 \pm 0.39) \times 10^{-8} \\ \mathcal{B}(h \to \phi\tau^+\tau^-) &= (2.35 \pm 0.12) \times 10^{-6} \\ \mathcal{B}(h \to J/\psi\mu^+\mu^-) &= (9.10 \pm 0.50) \times 10^{-8} \\ \mathcal{B}(h \to J/\psi\tau^+\tau^-) &= (1.82 \pm 0.10) \times 10^{-6} \\ \mathcal{B}(h \to \Upsilon\mu^+\mu^-) &= (5.60 \pm 0.37) \times 10^{-7} \\ \mathcal{B}(h \to \Upsilon\tau^+\tau^-) &= (5.66 \pm 0.29) \times 10^{-7}. \end{aligned} \tag{14}$$

The errors in the branching ratios include the uncertainties on the LCDA parameters, on the decay constants f_V and on the ratios R_{f_V} in Eqs. (11), and the error on $\mathcal{B}(h \to \gamma\gamma)_{exp}$. The uncertainties on f_V and on the meson LCDA parameters give a small contribution to the errors in (14), which are instead dominated by the uncertainty on $\mathcal{B}(h \to \gamma\gamma)_{exp}$ amounting to 50–60% of the total error, for the various channels. The uncertainty on R_{f_V} constitutes 20–30% of the total error. The uncertainty from the α_s corrections is not included in the error budget.

The larger rates in (14) are predicted for modes with τ pairs, $h \to \phi\tau^+\tau^-$ and $h \to J/\psi\tau^+\tau^-$. The modes with muons have rates suppressed by a factor 30 and 20, respectively, that could be experimentally overcome by the identification efficiency. In the case of Υ, the modes with $\tau^+\tau^-$ and $\mu^+\mu^-$ have similar branching fractions. Indeed, in both cases the dominant diagram is the one with two intermediate Z, Fig. 1(c) with practically coincident results. The next most relevant contribution is different: for $h \to \Upsilon\mu^+\mu^-$, it comes from the diagrams with the Higgs coupled to quarks, Fig. 1(a), while for $h \to \Upsilon\tau^+\tau^-$ it is with the Higgs coupled to leptons, Fig. 1(b). The two terms are almost equal in size in $h \to \Upsilon\mu^+\mu^-$ and $h \to \Upsilon\tau^+\tau^-$, respectively; the other diagrams give small contributions.

The branching fractions (14) can be compared to those predicted for $h \to V\gamma$: $\mathcal{B}(h \to \phi\gamma) = (2.31 \pm 0.11) \times 10^{-6}$ and $\mathcal{B}(h \to J/\psi\gamma) = (2.95 \pm 0.17) \times 10^{-6}$, while $\mathcal{B}(h \to \Upsilon\gamma)$ is $\mathcal{O}(10^{-9})$ [20]. For the $h \to VZ$ modes, $\mathcal{B}(h \to \phi Z) \simeq \mathcal{B}(h \to J/\psi Z) = 2.2 \times 10^{-6}$ are expected in SM [19].

The decay distributions in the normalized dilepton mass squared $\hat{q}^2 = q^2/m_h^2$, Fig. 2, show that the modes with final $\mu^+\mu^-$ pair and those with Υ are dominated by the virtual photon and Z contributions in Fig. 1(c). At a high luminosity facility, such ranges of $\hat{q}^2$ could be cut in the experimental analysis, to isolate the interferences among the various amplitudes. The forward–backward lepton asymmetry is tiny in the whole range of $\hat{q}^2$. For $h \to \phi\tau^+\tau^-$ and $h \to J/\psi\tau^+\tau^-$ the $\hat{q}^2$ distributions, in addition to the Z peak, are enhanced at large dilepton invariant mass, an effect of the diagrams with the Higgs coupled to the leptons.

The distributions of the fractions of longitudinally polarized vector meson $F_L(\hat{q}^2) = \frac{d\Gamma_L(h \to V\ell^+\ell^-)/d\hat{q}^2}{d\Gamma(h \to V\ell^+\ell^-)/d\hat{q}^2}$ are depicted in Fig. 3. Narrow peaks are found in $\phi\tau^+\tau^-$ and $J/\psi\tau^+\tau^-$, in correspondence to the intermediate Z, while in the other cases the $\hat{q}^2$ dependence is milder. For modes with $\mu^+\mu^-$ one has $F_L \simeq 1$ at the Z peak, where Z is almost completely longitudinally polarized since both the leptons, in the massless limit, have spins aligned to the direction of the motion.

The $h \to 4\ell$ modes, with $\ell = e, \mu$, have been analyzed in a kinematical region not far from the intermediate vector resonances, considering only the $h \to ZZ$ contribution, with the purpose of determining the difference in the dilepton spectra in SM and in possible extensions [34,35]. In particular, a correlation between the channels $h \to 2e2\mu$ and $h \to 4e(4\mu)$ has been recognized as an observable useful to identify the Higgs as a massive excitation of a $SU(2)_L$ doublet, and to probe the lepton flavor universality of possible NP contributions [35]. In our analysis we have

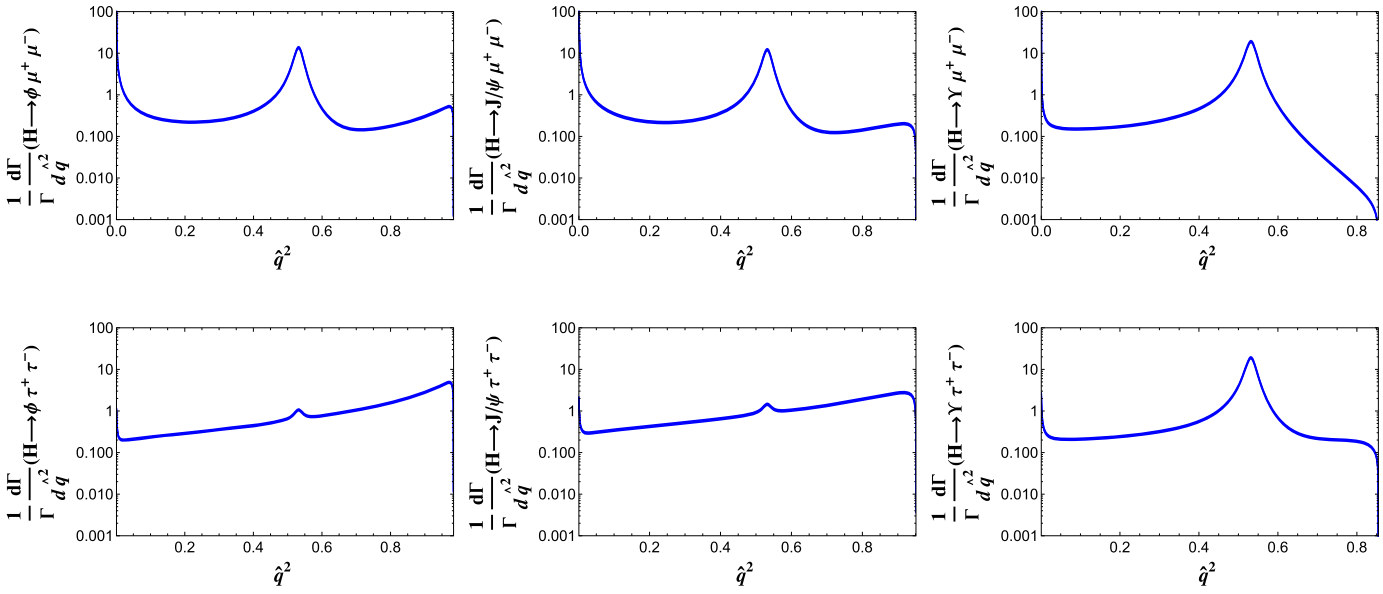

Fig. 2. Normalized decay distributions $(1/\Gamma)\, d\Gamma(h \to V\ell^+\ell^-)/d\hat{q}^2$, with $\hat{q}^2 = \frac{q^2}{m_h^2}$ and q^2 the dilepton mass squared.

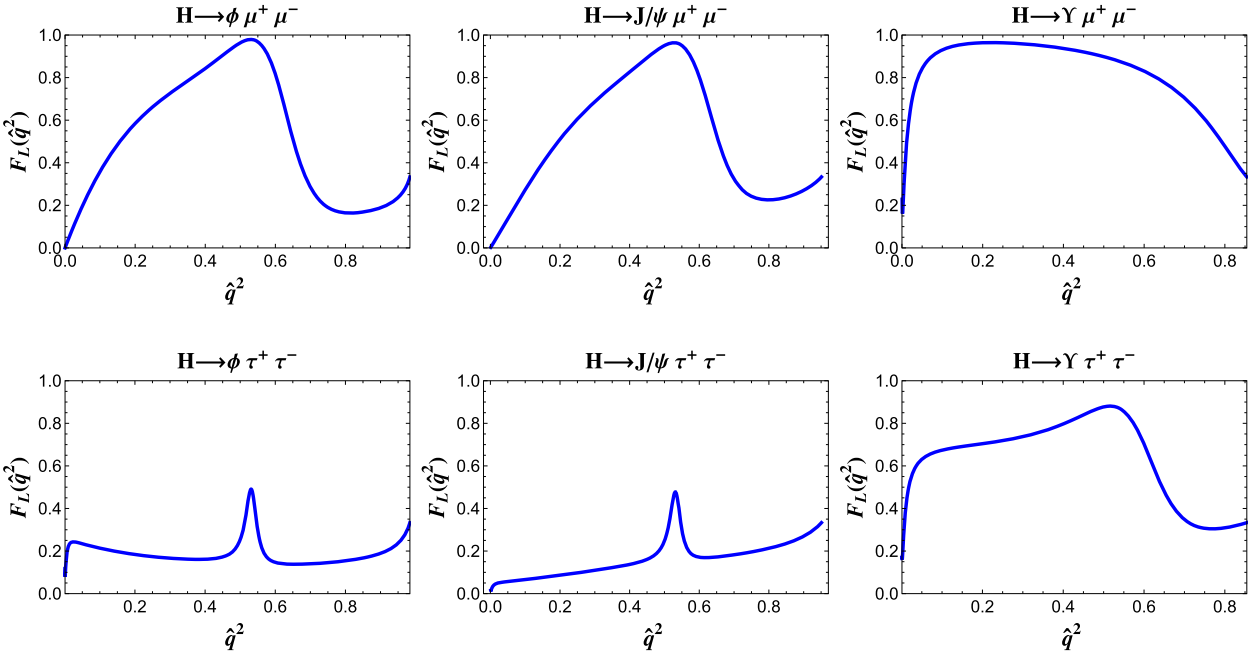

Fig. 3. Fraction $F_L(\hat{q}^2)$ of longitudinally polarized meson.

included the other diagrams; furthermore, we have studied the modes with τ leptons in SM.

The $h \to V\nu\bar{\nu}$ decay widths can be computed with appropriate changes in diagrams in Fig. 1, predicting

$$\begin{aligned} \mathcal{B}(h \to \phi\nu\bar{\nu}) &= (1.50 \pm 0.075) \times 10^{-7} \\ \mathcal{B}(h \to J/\psi\nu\bar{\nu}) &= (1.54 \pm 0.085) \times 10^{-7} \\ \mathcal{B}(h \to \Upsilon\nu\bar{\nu}) &= (1.52 \pm 0.08) \times 10^{-6} \ , \end{aligned} \tag{15}$$

with a factor 3 included to account for the neutrino species.

Finally, it is interesting to consider the implications of the LHC studies concerning the lepton flavor violating process $h \to \tau\mu$ on the exclusive $h \to V\tau\mu$ processes. The CMS results correspond to the effective coupling $\kappa_{h\tau\mu} = (2.6 \pm 0.6) \times 10^{-3}$, considering the uncertainties on $\mathcal{B}(h \to \tau^+\mu^-)$ and $\mathcal{B}(h \to \gamma\gamma)$. On the other hand, the ATLAS bound corresponds to $\kappa_{h\tau\mu} < 3.9 \times 10^{-3}$. For these values, the exclusive $h \to V\tau^+\mu^-$ branching fractions and their upper bounds can be computed from the diagrams in Fig. 1(b):

$$\begin{aligned} \mathcal{B}(h \to \phi\tau^+\mu^-) &= (3.2 \pm 1.5) \times 10^{-7} \ \ (< 6.9 \times 10^{-7}) \\ \mathcal{B}(h \to J/\psi\tau^+\mu^-) &= (2.4 \pm 1.1) \times 10^{-7} \ \ (< 5.2 \times 10^{-7}) \\ \mathcal{B}(h \to \Upsilon\tau^+\mu^-) &= (7.2 \pm 3.4) \times 10^{-9} \ \ (< 1.6 \times 10^{-8}) \ . \end{aligned} \tag{16}$$

The decay distributions in Fig. 4 have an enhancement at large q^2.

In conclusion, for our set of exclusive $h \to V\ell^+\ell^-$ decay modes the obtained branching ratios are in the range 10^{-8}–10^{-6} in SM, similar to $h \to \phi\gamma$, $h \to \Upsilon\gamma$, $h \to (\phi, J/\psi)\, Z$. The largest rate

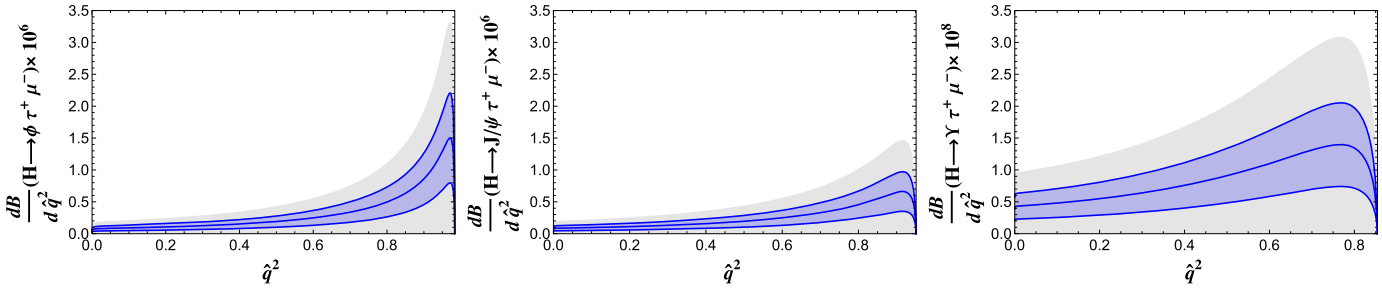

Fig. 4. Distributions $d\mathcal{B}(h \to V\tau^+\mu^-)/d\hat{q}^2$ obtained in correspondence to the CMS result for $\mathcal{B}(h \to \tau^+\mu^-)$ [10]. The light shaded area corresponds to the ATLAS bound in [11].

is for $h \to \phi\tau^+\tau^-$. In the differential $\hat{q}^2$ distributions the resonant structures at low q^2 and at $q^2 = m_Z^2$ are recognized, together with an enhancement at the q^2 end-point in $h \to \phi\tau^+\tau^-$ and $h \to J/\psi\tau^+\tau^-$. The rates of the neutrino modes have been predicted, the largest one is for Υ. We have also examined the implications of CMS and ATLAS results on the lepton flavor-changing process $h \to V\tau\mu$. These analyses confirm the role of the exclusive Higgs boson decays as precision tests of the Standard Model and important probes of physics beyond SM.

Acknowledgement

One of us (PC) thanks A. Khodjamirian for discussions.

Appendix A. Decay amplitudes

To give the expressions of the amplitudes corresponding to the diagrams in Fig. 1, we define

$$C_\gamma = 4\pi\alpha\, Q_\ell Q_q\,, \qquad C_Z = \frac{4\pi\alpha}{s_W^2 c_W^2}\,, \tag{17}$$

with $s_W = \sin\theta_W$, $c_W = \cos\theta_W$, and θ_W the Weinberg angle, and write the propagators in Fig. 1 in terms of the functions

$$\begin{aligned} D_1(a,b,\hat{q}^2) &= a + b\hat{q}^2 - ab\,\hat{m}_V^2 - \hat{m}_q^2\,,\\ D_2(\hat{q}^2) &= \hat{q}^2 - \hat{m}_Z^2 + i\,\hat{m}_Z\hat{\Gamma}_Z\,;\\ D_3(\hat{k}) &= 1 - 2n\cdot\hat{k}\,, \end{aligned} \tag{18}$$

where $n = (1,\vec{0})$ and we use the notation $\hat{x} = x/m_h$, x being a mass or a momentum. The factorized lepton current has various Dirac structures. Diagrams with intermediate photons involve the vector current

$$V_\ell^\mu = \bar{\psi}_\ell(k_1)\gamma^\mu\psi_{\bar{\ell}}(k_2) \tag{19}$$

while, diagrams with intermediate Z also involve

$$\begin{aligned} A_\ell^\mu &= \bar{\psi}_\ell(k_1)\gamma^\mu\gamma_5\psi_{\bar{\ell}}(k_2)\,,\\ T_\ell^{\mu\nu} &= \bar{\psi}_\ell(k_1)\gamma^\mu\gamma^\nu\psi_{\bar{\ell}}(k_2)\,,\\ \tilde{T}_\ell^{\mu\nu} &= \bar{\psi}_\ell(k_1)\gamma^\mu\gamma^\nu\gamma_5\psi_{\bar{\ell}}(k_2)\,. \end{aligned} \tag{20}$$

We write the SM neutral current coupled to the Z boson as

$$\mathcal{L}_\mu = \left(-\frac{ie}{s_W c_W}\right)\left(\Delta_V^f\,\bar{f}\gamma_\mu f + \Delta_A^f\,\bar{f}\gamma_\mu\gamma_5 f\right) \tag{21}$$

where f generically denotes a fermion, and

$$\Delta_V^f = \frac{1}{2}\left(T_3^f - 2s_W^2\,Q^f\right)\,, \qquad \Delta_A^f = -\frac{1}{2}T_3^f\,, \tag{22}$$

with T_3^f the third component of the weak isospin and Q^f the electric charge of f. Diagrams in Fig. 1(a) also involve the integrals over the LCDA of the vector meson V:

$$\begin{aligned} I_1 &= I_1(\hat{q}^2)\\ &= \int_0^1 du\,\phi_\perp^V(u)\left[\frac{1}{D_1(1-u,u,\hat{q}^2)} + \frac{1}{D_1(u,1-u,\hat{q}^2)}\right], \end{aligned} \tag{23}$$

$$\begin{aligned} I_2 &= I_1(\hat{q}^2)\\ &= \int_0^1 du\,\phi_\perp^V(u)\left[\frac{u}{D_1(1-u,u,\hat{q}^2)} + \frac{1-u}{D_1(u,1-u,\hat{q}^2)}\right]. \end{aligned} \tag{24}$$

With these definitions, the amplitudes in Fig. 1 can be written. We report the various expressions in correspondence with the diagrams in Fig. 1(a), (b) and (c), considering separately the intermediate photon and Z contributions.

- Fig. 1(a), intermediate γ:

$$A_{(a)}^\gamma = C_{(a)}^\gamma m_h \epsilon_V^{*\alpha} V_{\ell\mu}\left\{[n_\alpha \hat{p}_V^\mu - g_\alpha^\mu (n\cdot\hat{p}_V)]I_1 - g_\alpha^\mu \hat{m}_V^2 I_2\right\} \tag{25}$$

with

$$C_{(a)}^\gamma = \frac{1}{m_h^2}\frac{\hat{m}_q}{v} C_\gamma f_V^\perp \frac{1}{\hat{q}^2}\,. \tag{26}$$

- Fig. 1(a), intermediate Z:

$$\begin{aligned} A_{(a)}^Z = C_{(a)}^Z \epsilon_V^{*\alpha}&\left[\Delta_V^\ell\, V_{\ell\mu} + \Delta_A^\ell\, A_{\ell\mu}\right]\left(g^{\mu\alpha}p_V^\sigma - g^{\alpha\sigma}p_V^\mu\right)\\ &\times\left[n_\sigma I_1 - \hat{p}_{V\sigma} I_2\right] \end{aligned} \tag{27}$$

with

$$C_{(a)}^Z = -\frac{1}{m_h^2}\frac{\hat{m}_q}{v} C_Z \frac{1}{D_2(\hat{q}^2)} f_V^\perp\,\Delta_V^q\,. \tag{28}$$

- Fig. 1(b), intermediate γ:

$$A_{(b)}^\gamma = C_{(b)}^\gamma \epsilon_V^{*\alpha} n^\mu\left[-\frac{1}{D_3(\hat{k}_1)}\,T_{\ell\mu\alpha} + \frac{1}{D_3(\hat{k}_2)}\,T_{\ell\alpha\mu}\right] \tag{29}$$

with

$$C_{(b)}^\gamma = \frac{1}{m_h^2}\frac{\hat{m}_\ell}{v} C_\gamma \frac{f_V m_V}{\hat{m}_V^2}\,. \tag{30}$$

- Fig. 1(b), intermediate Z:

$$A^Z_{(b)} = C^Z_{(b)} \epsilon^*_{V\alpha} n_\mu \left\{ -\frac{1}{D_3(\hat{k}_1)} \left[\Delta^\ell_V T^{\mu\alpha}_\ell + \Delta^\ell_A \tilde{T}^{\mu\alpha}_\ell \right] + \frac{1}{D_3(\hat{k}_2)} \left[\Delta^\ell_V T^{\alpha\mu}_\ell - \Delta^\ell_A \tilde{T}^{\alpha\mu}_\ell \right] \right\} \tag{31}$$

with

$$C^Z_{(b)} = \frac{1}{m_h^2} \frac{\hat{m}_\ell}{v} C_Z \frac{\Delta^q_V}{D_2(\hat{m}^2_V)} f_V m_V \ . \tag{32}$$

- Fig. 1(c), two intermediate photons:

$$A^{\gamma\gamma}_{(c)} = C^{\gamma\gamma}_{(c)} \epsilon^{*\alpha}_V [g_{\alpha\mu}(q\cdot p_V) - m_h^2 n_\alpha n_\mu] V^\mu_\ell \tag{33}$$

with

$$C^{\gamma\gamma}_{(c)} = \frac{1}{m_h^4} \frac{\alpha}{\pi v} C_{\gamma\gamma} C_\gamma \frac{f_V m_V}{\hat{m}^2_V} \frac{1}{\hat{q}^2} \ . \tag{34}$$

- Fig. 1(c), two intermediate Z:

$$A^{ZZ}_{(c)} = C^{ZZ}_{(c)} \epsilon^*_{V\alpha} \left(\Delta^\ell_V V^\alpha_\ell + \Delta^\ell_A A^\alpha_\ell \right) \tag{35}$$

with

$$C^{ZZ}_{(c)} = \frac{1}{m_h^2} \frac{2\hat{m}^2_Z}{v} C_Z \frac{1}{D_2(\hat{q}^2)} \frac{1}{D_2(\hat{m}^2_V)} \Delta^q_V f_V m_V \ . \tag{36}$$

- Fig. 1(c), intermediate γZ, with γ converting to leptons:

$$A^{\gamma Z}_{(c)} = C^{\gamma Z}_{(c)} \epsilon^{*\alpha}_V [g_{\alpha\mu}(q\cdot p_V) - m_h^2 n_\alpha n_\mu] V^\mu_\ell \tag{37}$$

with

$$C^{\gamma Z}_{(c)} = \frac{1}{m_h^4} \frac{\alpha}{\pi v} C_{\gamma Z} \frac{4\pi\alpha Q_\ell}{s_W c_W} \frac{1}{\hat{q}^2} \frac{\Delta^q_V}{D_2(\hat{m}^2_V)} f_V m_V \ . \tag{38}$$

- Fig. 1(c), intermediate $Z\gamma$, with Z converting to leptons:

$$A^{Z\gamma}_{(c)} = C^{Z\gamma}_{(c)} \epsilon^{*\alpha}_V [g_{\alpha\mu}(q\cdot p_V) - m_h^2 n_\alpha n_\mu] \left(\Delta^\ell_V V^\mu_\ell + \Delta^\ell_A A^\mu_\ell \right) \tag{39}$$

with

$$C^{Z\gamma}_{(c)} = \frac{1}{m_h^4} \frac{\alpha}{\pi v} C_{\gamma Z} \frac{4\pi\alpha Q_q}{s_W c_W} \frac{1}{\hat{m}^2_V} \frac{1}{D_2(\hat{q}^2)} f_V m_V \ . \tag{40}$$

The effective couplings $C_{\gamma\gamma}$ and $C_{\gamma Z}$ are defined through Eq. (12).

References

[1] ATLAS Collaboration, G. Aad, et al., Observation of a new particle in the search for the standard model Higgs boson with the ATLAS detector at the LHC, Phys. Lett. B 716 (2012) 1–29, arXiv:1207.7214.

[2] CMS Collaboration, S. Chatrchyan, et al., Observation of a new boson at a mass of 125 GeV with the CMS experiment at the LHC, Phys. Lett. B 716 (2012) 30–61, arXiv:1207.7235.

[3] Particle Data Group Collaboration, K.A. Olive, et al., Review of particle physics, Chin. Phys. C 38 (2014) 090001.

[4] ATLAS and CMS, Measurements of the Higgs boson production and decay rates and constraints on its couplings from a combined ATLAS and CMS analysis of the LHC pp collision data at $\sqrt{s} = 7$ and 8 TeV, ATLAS-CONF-2015-044, CMS-PAS-HIG-15-002.

[5] R. Contino, M. Ghezzi, C. Grojean, M. Muhlleitner, M. Spira, Effective Lagrangian for a light Higgs-like scalar, J. High Energy Phys. 07 (2013) 035, arXiv:1303.3876.

[6] I. Brivio, T. Corbett, O.J.P. Éboli, M.B. Gavela, J. Gonzalez-Fraile, M.C. Gonzalez-Garcia, L. Merlo, S. Rigolin, Disentangling a dynamical Higgs, J. High Energy Phys. 03 (2014) 024, arXiv:1311.1823.

[7] M. Gonzalez-Alonso, A. Greljo, G. Isidori, D. Marzocca, Pseudo-observables in Higgs decays, Eur. Phys. J. C 75 (2015) 128, arXiv:1412.6038.

[8] R.S. Gupta, A. Pomarol, F. Riva, BSM primary effects, Phys. Rev. D 91 (3) (2015) 035001, arXiv:1405.0181.

[9] Y.T. Chien, V. Cirigliano, W. Dekens, J. de Vries, E. Mereghetti, Direct and indirect constraints on CP-violating Higgs-quark and Higgs-gluon interactions, arXiv:1510.00725.

[10] CMS Collaboration, V. Khachatryan, et al., Search for lepton-flavour-violating decays of the Higgs boson, Phys. Lett. B 749 (2015) 337–362, arXiv:1502.07400.

[11] ATLAS Collaboration, G. Aad, et al., Search for lepton-flavour-violating $H \to \mu\tau$ decays of the Higgs boson with the ATLAS detector, J. High Energy Phys. 11 (2015) 211, arXiv:1508.03372.

[12] A. Abbasabadi, D. Bowser-Chao, D.A. Dicus, W.W. Repko, Radiative Higgs boson decays H → fermion anti-fermion gamma, Phys. Rev. D 55 (1997) 5647–5656, arXiv:hep-ph/9611209.

[13] L.-B. Chen, C.-F. Qiao, R.-L. Zhu, Reconstructing the 125 GeV SM Higgs boson through $\ell\bar{\ell}\gamma$, Phys. Lett. B 726 (2013) 306–311, arXiv:1211.6058.

[14] Y. Sun, H.-R. Chang, D.-N. Gao, Higgs decays to gamma l^+l^- in the standard model, J. High Energy Phys. 05 (2013) 061, arXiv:1303.2230.

[15] D.A. Dicus, W.W. Repko, Calculation of the decay $H \to e\bar{e}\gamma$, Phys. Rev. D 87 (7) (2013) 077301, arXiv:1302.2159.

[16] G. Passarino, Higgs boson production and decay: Dalitz sector, Phys. Lett. B 727 (2013) 424–431, arXiv:1308.0422.

[17] G.T. Bodwin, F. Petriello, S. Stoynev, M. Velasco, Higgs boson decays to quarkonia and the $H\bar{c}c$ coupling, Phys. Rev. D 88 (5) (2013) 053003, arXiv:1306.5770.

[18] A.L. Kagan, G. Perez, F. Petriello, Y. Soreq, S. Stoynev, J. Zupan, Exclusive window onto Higgs Yukawa couplings, Phys. Rev. Lett. 114 (10) (2015) 101802, arXiv:1406.1722.

[19] G. Isidori, A.V. Manohar, M. Trott, Probing the nature of the Higgs-like boson via $h \to V\mathcal{F}$ decays, Phys. Lett. B 728 (2014) 131–135, arXiv:1305.0663.

[20] M. Koenig, M. Neubert, Exclusive radiative Higgs decays as probes of light-quark Yukawa couplings, J. High Energy Phys. 08 (2015) 012, arXiv:1505.03870.

[21] B. Bhattacharya, A. Datta, D. London, Probing new physics in Higgs couplings to fermions using an angular analysis, Phys. Lett. B 736 (2014) 421–427, arXiv:1407.0695.

[22] D.-N. Gao, A note on Higgs decays into Z boson and $J/\psi(\Upsilon)$, Phys. Lett. B 737 (2014) 366–368, arXiv:1406.7102.

[23] G.P. Lepage, S.J. Brodsky, Exclusive processes in quantum chromodynamics: evolution equations for hadronic wave functions and the form-factors of mesons, Phys. Lett. B 87 (1979) 359–365.

[24] G.P. Lepage, S.J. Brodsky, Exclusive processes in perturbative quantum chromodynamics, Phys. Rev. D 22 (1980) 2157.

[25] A.V. Efremov, A.V. Radyushkin, Factorization and asymptotical behavior of pion form-factor in QCD, Phys. Lett. B 94 (1980) 245–250.

[26] V.L. Chernyak, A.R. Zhitnitsky, Asymptotic behavior of exclusive processes in QCD, Phys. Rep. 112 (1984) 173.

[27] P. Ball, G.W. Jones, R. Zwicky, B → V gamma beyond QCD factorisation, Phys. Rev. D 75 (2007) 054004, arXiv:hep-ph/0612081.

[28] P. Ball, G.W. Jones, Twist-3 distribution amplitudes of K* and phi mesons, J. High Energy Phys. 03 (2007) 069, arXiv:hep-ph/0702100.

[29] Y. Grossman, M. Koenig, M. Neubert, Exclusive radiative decays of W and Z bosons in QCD factorization, J. High Energy Phys. 04 (2015) 101, arXiv:1501.06569.

[30] P. Ball, V.M. Braun, Higher twist distribution amplitudes of vector mesons in QCD: twist – 4 distributions and meson mass corrections, Nucl. Phys. B 543 (1999) 201–238, arXiv:hep-ph/9810475.

[31] W.E. Caswell, G.P. Lepage, Effective Lagrangians for bound state problems in QED, QCD, and other field theories, Phys. Lett. B 167 (1986) 437–442.

[32] G.T. Bodwin, E. Braaten, G.P. Lepage, Rigorous QCD analysis of inclusive annihilation and production of heavy quarkonium, Phys. Rev. D 51 (1995) 1125–1171, arXiv:hep-ph/9407339; Erratum, Phys. Rev. D 55 (1997) 5853.

[33] LHC Higgs Cross Section Working Group Collaboration, J.R. Andersen, et al., Handbook of LHC Higgs cross sections: 3. Higgs properties, arXiv:1307.1347.

[34] M. Gonzalez-Alonso, G. Isidori, The $h \to 4l$ spectrum at low m_{34}: standard model vs. light new physics, Phys. Lett. B 733 (2014) 359–365, arXiv:1403.2648.

[35] M. Gonzalez-Alonso, A. Greljo, G. Isidori, D. Marzocca, Electroweak bounds on Higgs pseudo-observables and $h \to 4\ell$ decays, Eur. Phys. J. C 75 (2015) 341, arXiv:1504.04018.